Available online at www.sciencedirect.com
ScienceDirect
Free Radical Biology & Medicine 42 (2007) 1496–1505
www.elsevier.com/locate/freeradbiomed

Original Contribution

Thioredoxin-linked metabolism in *Entamoeba histolytica*

Diego G. Arias [a,b], César E. Gutierrez [a], Alberto A. Iglesias [b], Sergio A. Guerrero [a,*]

[a] *Laboratorio de Bioquímica Microbiana, Facultad de Bioquímica y Ciencias Biológicas, Universidad Nacional del Litoral, Ciudad Universitaria–Paraje El Pozo, 3000 Santa Fe, Argentina*
[b] *Laboratorio de Enzimología Molecular, Facultad de Bioquímica y Ciencias Biológicas, Universidad Nacional del Litoral, Ciudad Universitaria–Paraje El Pozo, 3000 Santa Fe, Argentina*

Received 21 September 2006; revised 15 January 2007; accepted 8 February 2007
Available online 20 February 2007

Abstract

Entamoeba histolytica, an intestinal protozoan that is the causative agent of amoebiasis, is exposed to elevated amounts of highly toxic reactive oxygen species during tissue invasion. In this work, we report the molecular cloning, from *E. histolytica* genomic DNA, of the genes *ehtrxr* and *ehtrx41*, respectively coding for thioredoxin reductase (*Eh*TRXR) and thioredoxin (*Eh*TRX41). The genes were expressed in *Escherichia coli* cells, and the corresponding recombinant proteins were purified and characterized. *Eh*TRXR catalyzed the NADPH (K_m=4.5 μM)-dependent reduction of 5,5′-dithiobis-(2-nitrobenzoic) acid (K_m=1.7 mM), *Eh*TRX41 (K_m=3.6 μM), and *E. coli* TRX (K_m=4.6 μM). *Eh*TRXR and *Eh*TRX41 could be assayed as a functional redox pair that, together with peroxiredoxin, mediate the NADPH-dependent reduction of hydrogen peroxide and *tert*-butyl hydroperoxide. It is proposed that this detoxifying system could be operative in vivo. Results add value to the genome project information and advise reconsideration of key metabolic pathways operating in *E. histolytica*.

Keywords: *Entamoeba histolytica*; Redox metabolism; Thioredoxin system; Structural and functional characterization; Free radicals

Amoebiasis is an intestinal infection widespread throughout the world caused by the human pathogen *Entamoeba histolytica.* Many people, mainly in developing countries, suffer chronically from this disease, from which morbidity and mortality are high in poor populations and cause substantial economic burden on public health [1]. Identification of specific molecular targets is relevant to designing new therapeutic drugs for improvement of the treatment of this disease [2]. For this, characterization of the physiology and biochemistry of the pathogen is a critical issue, with those processes involved in redox metabolism being of particular interest. The recent elucidation of the genome of *E. histolytica* affords a key tool to identify the occurrence and operation of different metabolisms in the parasite [3].

It is known that the trofozoites of *E. histolytica* find in the anaerobic environment of the human gut a suitable place to live and multiply. However, during tissue invasion the microorganism is exposed to relatively high oxygen pressure and, consequently, to environments containing high levels of reactive oxygen species (ROS) [such as superoxide radical anions ($O_2^{\bullet -}$) and hydrogen peroxide (H_2O_2)]. Earlier studies indicated that the parasite can tolerate up to 5% oxygen in the gas phase [3–5]. Distinctively, *E. histolytica* is a eukaryote lacking or having quantitatively insignificant amounts of glutathione and its associated enzymes [6,7]. In addition, the occurrence of trypanothione metabolism in the parasite is the subject of several studies [2,6,8–10].

In a recent analysis performed to study the *E. histolytica* genome [3], the molecular components involved in redox metabolism and in oxidative stress response were considered. These included and were limited to: (i) the metabolite cysteine [11,12], the major intracellular thiol, high levels of which in the parasite are thought to compensate for the lack of glutathione; (ii) the enzyme Fe-superoxide dismutase (FeSOD) [13,14]; (iii) flavoprotein A, which with the respective reductase is involved

Abbreviations: ROS, reactive oxygen species; TRXR, thioredoxin reductase; TRX, thioredoxin; *Eh*p29, peroxiredoxin; DTNB, 5,5′-dithiobis(2-nitrobenzoic acid); DTT, dithiothreitol; *t*-BOOH, *tert*-butyl hydroperoxide.

* Corresponding author. Fax: +54 342 457 5221.
E-mail address: sguerrer@fbcb.unl.edu.ar (S.A. Guerrero).

0891-5849/$ - see front matter © 2007 Published by Elsevier Inc.
doi:10.1016/j.freeradbiomed.2007.02.012

in oxygen and nitric oxide detoxification [3]; (iv) rubrerythrin, a protein also found in anaerobic bacteria [3]; (v) a 29-kDa protein, peroxiredoxin (*Eh*p29) [4,15,16]; and (vi) a 34-kDa protein characterized as NADPH oxidase (EC 1.5.1.30) [17,18], also exhibiting a secondary NADPH-dependent oxidoreductase activity [18].

All forms of life have developed efficient enzymatic systems to resist the oxidative damage generated by ROS and to maintain the intracellular redox balance. One of these, the thioredoxin reductase (TRXR)/thioredoxin (TRX) system, utilizes reduction equivalents from NADPH and is involved in different biological processes such as protection against oxidative stress, regulation of DNA synthesis, transcription, cellular growth, and apoptosis. The system ultimately functions as a donor of reducing equivalents for various bioprocesses and has been found widespread in different organisms, including unicellular parasites [19–21]. Here, we report on the molecular cloning of two genes from *E. histolytica* encoding TRXR and TRX, respectively, as well as the expression, purification, and functional characterization of both recombinant proteins. To the best of our knowledge, this is the first time that the occurrence of a TRXR/TRX system has been identified in this parasite, by which this work contributes to the functional genomic and proteomic of *E. histolytica*, and it mainly highlights that the redox metabolic scenario in this organism needs to be revisited.

Materials and methods

Materials

Bacteriological media components were from Britania Laboratories (Rosario, Argentina). *Taq* DNA polymerase and the restriction enzymes were from Promega. All other reagents and chemicals were of the highest quality commercially available.

Bacteria and plasmids

Escherichia coli Top 10 cells (Invitrogen) and *E. coli* BL21 (DE3) were utilized in routine plasmid construction and expression experiments. The vector pGEM-T Easy (Promega) was selected for cloning and sequencing purposes. The expression vector was pRSET-A (Invitrogen). Cells and genomic DNA from *E. histolytica* (strain HM1-IMSS) were kindly provided by Dr. Hugo Luján (INIMEC-CONICET, Universidad Nacional de Córdoba, Argentina). DNA manipulation, *E. coli* culture, and transformation were performed according to standard protocols [22].

Molecular cloning of trxr, trx41, and peroxiredoxin (p29) from E. histolytica

The genes were amplified from *E. histolytica* genomic DNA by PCR techniques. Oligonucleotide primer pairs utilized for PCR amplification were designed from reported spliced sequences (Wellcome Trust, Sanger Institute, Pathogen Sequencing Unit, http://www.genedb.org/), as described in Table 1.

Table 1
Primers used for amplifying the genes encoding thioredoxin reductase (*Eh*TRXR), thioredoxin (*Eh*TRX), and peroxiredoxin (*Eh*p29)

Primer	Oligonucleotide	Restriction site	T_m (°C)
TRXRfow	GGATCCATGAGTAATATTCATGATGT	*Bam*HI	63.4
TRXRrev	AAGCTTATGAGTTTGAAGCCATTTTTC	*Hin*dIII	69.2
TRX41fow	GGATCCATGTCTCTTATTCATTTAAATTC	*Bam*HI	64.3
TRX41rev	AAGCTTTTATTGAAAAGCAGCCCACA	*Hin*dIII	67.7
p29fow	GGATCCATGTCTTGCAATCAACAAAAAG	*Bam*HI	75.6
p29rev	AAGCTTTTAATGTGCTGTTAAATATT	*Hin*dIII	62.7

Primers were designed from the *Entamoeba histolytica* genome available at http://www.genedb.org. TRXRfow and TRXRrev were for trxr (CDS 23.m00296), TRX41fow and TRX41rev were for trx41 (CDS 41.m00230), p29fow and p29rev were for the fully characterized peroxiredoxin (CDS 298.m00058) [3,13,14].

Each PCR was performed under the following conditions: 94 °C for 10 min; 30 cycles of 94 °C for 1 min, 55 °C for 1 min, and 72 °C for 1 min; then 72 °C for 10 min. The PCR product was subsequently purified and ligated into the pGEM-T Easy vector (Promega) to facilitate further work. The fidelity and correctness of each gene were confirmed on both strands by complete sequencing.

Construction of the expression vectors

The constructions obtained as described above (into pGEM-T Easy system) and the pRSET-A vector (Invitrogen) were digested with the enzymes *Bam*HI and *Hin*dIII. Restriction fragments were purified by gel extraction after gel electrophoresis. Ligation to the pRSET-A vector of each insert was performed using T4 DNA ligase for 16 h at 10 °C. Competent *E. coli* BL21(DE3) cells were transformed with the respective construct. Transformed cells were selected in agar plates containing Luria–Bertani broth (LB; 10 g/L NaCl, 5 g/L yeast extract, 10 g/L peptone, pH 7.4) supplemented with ampicillin (100 μg/ml). Preparation of plasmid DNA and subsequent *Bam*HI/*Hin*dIII restriction treatment were performed to check the correctness of the different constructs.

Overexpression and purification of the E. histolytica TRXR, TRX41, and p29 recombinant proteins

Single colonies of *E. coli* BL21(DE3) transformed with the respective recombinant plasmid were selected. Overnight cultures were diluted 1/100 in fresh medium (LB broth supplemented with 100 μg/ml ampicillin) and grown under identical conditions to exponential phase, OD_{600} of 0.6. The expression of the respective recombinant protein was induced with 0.5 mM IPTG, followed by incubation at 28 °C. After 16 h the cells were harvested and stored at −20 °C. Purification of each recombinant protein was performed using a Co^{2+}–IDA–agarose resin (Invitrogen). Briefly, the bacterial pellet was resuspended in binding buffer (20 mM Tris–HCl, pH 8.0, 100 mM NaCl) and disrupted by sonication. The lysate was centrifuged (10,000*g*, 30 min) to remove cell debris. The resultant crude extract was loaded onto a Co^{2+}–IDA–agarose

column that had been equilibrated with binding buffer. After being washed with 10 bead volumes of the same buffer, the recombinant protein was eluted with elution buffer (20 mM Tris–HCl, pH 8.0, 100 mM NaCl, 250 mM imidazole). Active fractions were pooled and precipitated with ammonium sulfate to 90% saturation and stored at 4 °C. In the case of peroxiredoxin, the purified recombinant protein was stored at 4 °C in 10 mM Tris–HCl, pH 8.0. Under the specified storage conditions, the recombinant proteins were stable for at least 6 months. His-tagged *E. coli* thioredoxin was purified from *E. coli* BL21(DE3) cells transformed with the commercial pET32a plasmid.

Protein methods

Cell-free extracts were analyzed by SDS–PAGE [23] using the Bio-Rad minigel apparatus. The final polyacrylamide monomer concentration was 15% (w/v) for the separating gel and 4% (w/v) for the stacking gel. Coomassie brilliant blue was used to stain protein bands. Protein contents were determined by the method of Bradford [24] with BSA as standard. Desalting was performed on Bio-Gel P chromatography columns (Bio-Rad).

Sera anti-*Eh*TRXR and anti-*Eh*TRX41 were prepared by rabbit immunization with the purified recombinant proteins according to Vaitukaitis et al. [25]. To obtain extracts from *E. hystolytica*, trophozoites were washed three times in 20 mM Tris–HCl, pH 7.5, 2 mM EDTA, and resuspended in the same buffer at a concentration of 3×10^7 cells/ml. The cells were disrupted by sonication. Detection of specific proteins by Western blotting was performed after standard techniques [22]. Proteins in SDS–PAGE gels were blotted onto PVDF membranes using a Mini-PROTEANII (Bio-Rad) apparatus. The membrane was blocked overnight at 4 °C, subsequently incubated with primary antibody at room temperature for 1 h, and then incubated with a HRP-conjugated anti-rabbit secondary antibody for 1 h. Detection was carried out with 3,3′-diaminobenzidine and hydrogen peroxide (Sigma) in 50 mM Tris–HCl, pH 8.0, 150 mM NaCl.

Enzyme assays

All the enzyme assays were performed at 25 °C, in a final volume of 250 µl, and using a Multiskan Ascent one-channel vertical light path filter photometer (Thermo Electron Co.). One unit (U) of activity is defined as the amount of enzyme which catalyzes the conversion of 1 µmol of substrate per minute under the conditions specified in each case.

TRXR activity was measured by monitoring the oxidation of NADPH at 340 nm in a reaction mixture comprising 100 mM potassium phosphate, pH 7.0, 2 mM EDTA, 0.2 mM NADPH, 0.13 mM bovine insulin, 0.15–30 µM TRXs, and 0.1–0.8 µM *Eh*TRXR. The reaction was started by the addition of *Eh*TRXR [20,26,27].

5,5′-Dithiobis(2-nitrobenzoic acid) (DTNB) reductase activity was measured by monitoring the production of thionitrobenzoate at 412 nm in a reaction mixture comprising 100 mM potassium phosphate, pH 7.0, 2 mM EDTA, 0.2 mM NADPH, 0.01–15 mM DTNB, and 0.1–0.8 µM *Eh*TRXR. Activity was calculated using the molar extinction coefficient at 412 nm of 13,600 M^{-1} cm^{-1} and considering that 1 mol of NADPH yields 2 mol of thionitrobenzoate [18,28].

NADPH oxidase activity was assayed by monitoring the oxidation of NADPH at 340 nm in reaction mixtures containing 100 mM potassium phosphate, pH 7.0, 2 mM EDTA, 0.2 mM NADPH, and 0.3–2 µM *Eh*TRXR [18,28].

Hydroperoxide detoxification activity was determined by monitoring the oxidation of NADPH at 340 nm, in a reaction mixture containing 100 mM potassium phosphate, pH 7.0, 2 mM EDTA, 0.4 mM NADPH, 1 µM *Eh*TRXR, 10–20 µM TRXs, 1 µM *Eh*p29 (1 U mg^{-1}), and 0.5 mM *tert*-butyl hydroperoxide (*t*-BOOH) as final acceptor [29].

TRX activity was measured by monitoring the reduction of insulin at 650 nm in a reaction mixture comprising 100 mM potassium phosphate, pH 7.0, 2 mM EDTA, 1 mM DTT, 0.13 mM insulin, and TRXs in concentrations from 1 to 9 µM [20,26,27].

Saturation curves were performed by assaying the respective enzyme activity at saturating level of fixed substrate and different concentrations (between 7 and 13 points) of the variable substrate. The kinetic data were plotted as initial velocity (µM min^{-1}) versus substrate concentration (µM or mM). The kinetic constants were acquired by fitting the data with a nonlinear least-squares formula and the Michaelis–Menten equation using the program Origin. Kinetic constants are the mean of at least three independent sets of data, and they are reproducible within ±10%.

Results

Isolation and characterization of the genes ehtrxr and ehtrx

The identification of a spliced nucleotide sequence (ehtrxr, CDS 23.m00296) encoding a putative TRXR in the database of the *E. histolytica* genome project (Wellcome Trust, Sanger Institute, Pathogen Sequencing Unit, http://www.genedb.org/) prompted us to perform the molecular cloning of the full-length ehtrxr. This gene was amplified from genomic DNA and its identity was confirmed by DNA sequencing. The gene (945 bp in length) is predicted to encode a 314-amino-acid protein (*Eh*TRXR) with a molecular mass of 33.7 kDa and a calculated *p*I of 5.94. The protein is similar in size to other members of the low-molecular-weight family of TRXR (L-TRXR) [30]. An alignment of the deduced *Eh*TRXR amino acid sequence with other L-TRXRs shows a high sequence identity and the presence in the former of the redox active site containing two key cysteine residues (Fig. 1).

Another spliced sequence of a gene coding for a putative TRX (CDS 41.m00230) was also identified in the *E. histolytica* genome project database. The full-length DNA fragment was amplified by PCR as described under Materials and methods and its identity confirmed by DNA sequencing. It is predicted that *ehtrxr* encodes a protein of 105 amino acids (*Eh*TRX41) with a molecular mass of 12.2 kDa and a calculated *p*I of 6.08. Fig. 2 shows an alignment of amino acid sequences between *Eh*TRX41

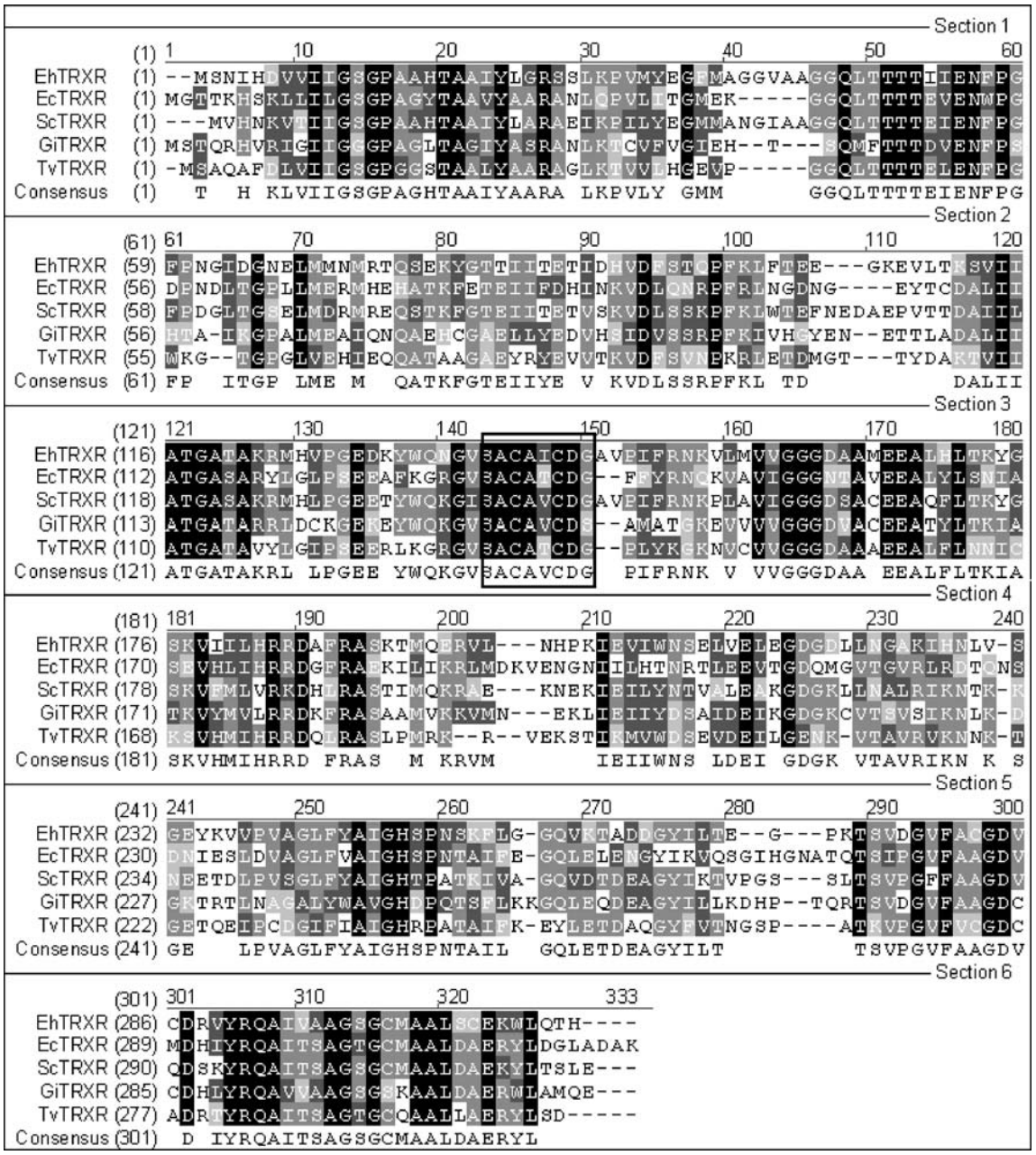

Fig. 1. Alignment of *E. histolytica* TRXR (this study) with homologues from *E. coli* (NCBI Accession No. BAA35613), *Saccharomyces cerevisiae* (NCBI Accession No. NP010640), *G. intestinalis* (NCBI Accession No. CAD47839), and *Trichomonas vaginalis* (NCBI Accession No. CAD47837). Each individual sequence is numbered accordingly.

and TRXs from different sources. The *E. histolytica* protein exhibited different degrees of identity with TRX from *Trichomonas vaginalis* (23%), *Trypanosoma cruzi* (27%), *E. coli* (21%), and *Homo sapiens* (36%). As also illustrated in Fig. 2, the amino acid sequence identity was complete at the WCGPCK motif, identified as the redox active site in TRXs [31].

Expression and characterization of recombinant EhTRXR and EhTRX41

To further seek the functionality of the proteins, the genes encoding *Eh*TRXR and *Eh*TRX41 were cloned into the prokaryotic expression vector pRSET-A. The expression in *E. coli* BL21(DE3) rendered recombinant proteins produced as polypeptides tagged with histidine residues at the N-terminus. The soluble fractions were purified chromatographically onto a Co^{2+}-affinity resin, to obtain recombinant proteins with purity higher than 90%, as judged by SDS–PAGE analysis shown in Fig. 3A. The molecular mass thus revealed for each protein, 36 kDa for *Eh*TRXR and 15 kDa for *Eh*TRX (Figs. 3A and 3B), fully agrees with the expected sizes deduced from their DNA-derived amino acid sequence plus ca. 3 kDa of the residues contained in the histidine tag. The same system was utilized to express *Eh*p29 (Fig. 3A), a peroxiredoxin previously

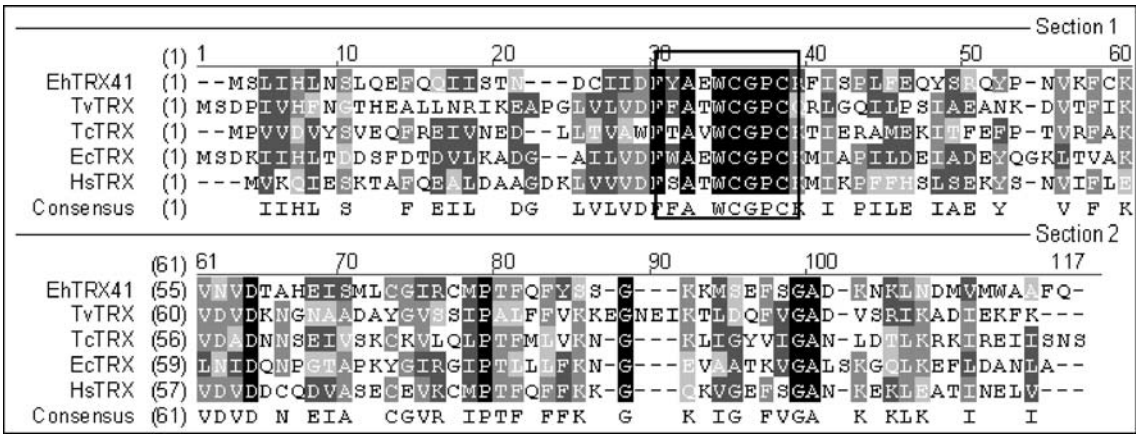

Fig. 2. Amino acid sequence alignment of *E. histolytica* TRX41 (this study) with homologues *Tri. vaginalis* TRX (NCBI Accession No. CAD47836), *Trypanosoma cruzi* TRX (NCBI Accession No. AAT79533), *E. coli* TRX (NCBI Accession No. M54881), and *Homo sapiens* TRX (NCBI Accession No. JH0568). Each individual sequence is numbered accordingly.

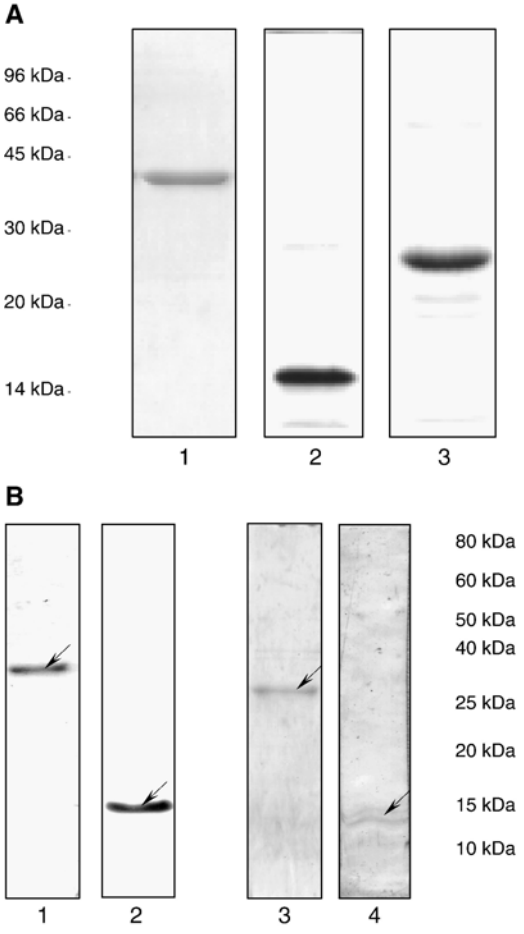

Fig. 3. (A) Electrophoretic analysis of the purified recombinant proteins. The proteins were defined by 15% (w/v) SDS–PAGE and stained with Coomassie blue. Lane 1, *Eh*TRXR (2 μg); lane 2, *Eh*TRX41 (4 μg); lane 3, *Eh*p29 (4 μg). (B) Western blotting. Lane 1, recombinant *Eh*TRXR (2 μg) revealed with rabbit polyclonal anti-*Eh*TRXR; lane 2, recombinant *Eh*TRX41 (2 μg) revealed with rabbit polyclonal anti-*Eh*TRX41; lane 3, *E. histolytica* crude extract from 5×10^5 cells revealed with rabbit polyclonal anti-*Eh*TRXR; and lane 4, *E. histolytica* crude extract from 5×10^5 cells revealed with rabbit polyclonal anti-*Eh*TRX41.

described as functional in the parasite [15,16]. We also searched for the occurrence of TRXR and TRX41 in cells of *E. histolytica* utilizing polyclonal antibodies raised against the respective recombinant protein. As illustrated in Fig. 3B, in Western blots of extracts of trophozoites protein bands of molecular masses about 12 and 33 kDa, which respectively correlate with recombinant *Eh*TRX41 and *Eh*TRXR, were visualized (Fig. 3B).

The purified recombinant proteins were analyzed with respect to their capacities to mediate redox reactions. *Eh*TRXR was active as NADPH oxidase, with increasing amounts of purified reductase in the assay medium giving increasing rates of NADPH oxidation (Fig. 4). Hyperbolic saturation kinetics for NADPH were observed, with K_m and V_{max} values estimated to be 3.6 μM and 0.37 $U \cdot mg^{-1}$ (inset Fig. 4). The formation of hydrogen peroxide associated with this reaction was confirmed by dosage with the ferrithiocyanate method [18] (data not shown). The protein was also analyzed for its ability to catalyze the reduction of a disulfide

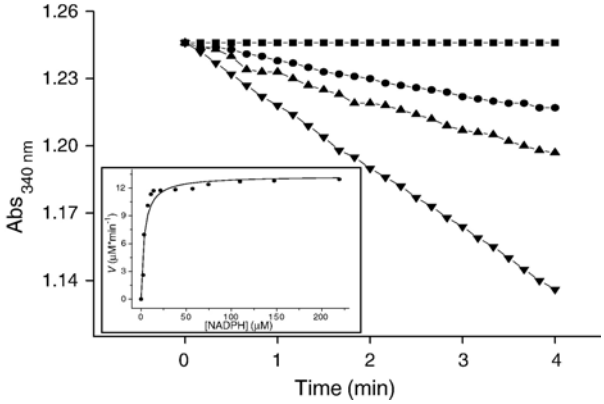

Fig. 4. NADPH oxidase activity of *Eh*TRXR. The reactions were performed in buffer (100 mM phosphate, pH 7.0, 2 mM EDTA), 200 μM NADPH, and the absence or presence of different concentrations of *Eh*TRXR: (■) no *Eh*TRXR; (●) 0.32 μM; (▲) 0.80 μM; (▼) 2.40 μM. Inset: saturation curve for NADPH utilizing 0.32 μM *Eh*TRXR.

compound such as DTNB. Fig. 5 illustrates that increasing rates of the NADPH-dependent DTNB reduction were observed at different *Eh*TRXR levels in the medium, ranging from 0.13 to 0.66 μM. In our hands, reduction of DTNB by *Eh*TRXR followed a hyperbolic behavior with K_m values of 1.7 mM (DTNB) and 4.5 μM (NADPH) and a V_{max} value of 0.33 U mg^{-1} (inset Fig. 5).

*Eh*TRX41 was also functional, as was determined by the insulin assay [20,26,27]. The method is based on the capacity of DTT-reduced TRX to reduce insulin, after which the β chain becomes insoluble and precipitates. As shown in Fig. 6, in the absence of TRX no increase in turbidity was observed at 650 nm after 30 min, whereas in the presence of purified *Eh*TRX41 (that had been chemically reduced by DTT) reduction of insulin was detectable after approximately 5 min of incubation. Moreover, the rate of insulin reduction was dependent on the amount of *Eh*TRX41 included in the assay medium (Fig. 6).

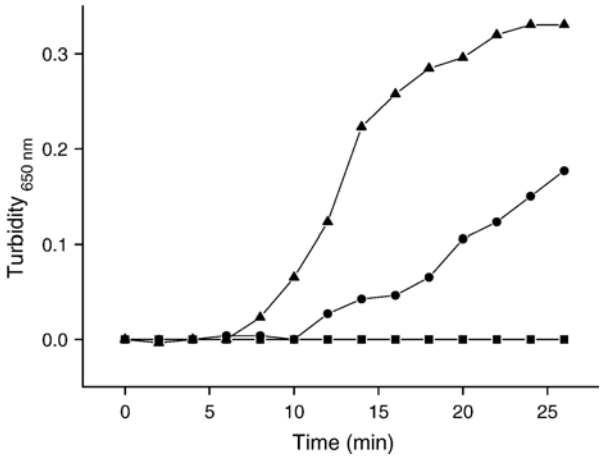

Fig. 6. Insulin reduction by recombinant *Eh*TRX41. The reactions were performed in buffer (100 mM phosphate, pH 7.0, 2 mM EDTA), 0.5 mM DTT, 130 μM insulin, and different concentrations of TRX: (■) no *Eh*TRX41; (●) *Eh*TRX41 1.5 μM; (▲) *Eh*TRX41 3 μM.

EhTRXR and EhTRX41 function as a redox system

To further characterize the functional capacity of the recombinant proteins we analyzed the behavior of *Eh*TRXR as a true reductase of TRXs. Fig. 7 shows that over the NADPH oxidase activity exhibited by *Eh*TRXR, the addition of *Eh*TRX41 and insulin increased the rate of NADPH oxidation. For such an increase, both of the components were necessary, as the addition of insulin alone produced no effect. These results were confirmed by determining the reduction of insulin after the increase in turbidity at 650 nm (data not shown). Results indicate that reduction of insulin by *Eh*TRX41 required the previous reduction of the protein by NADPH, which is catalyzed by *Eh*TRXR. Similar results were obtained with *E. coli* TRX (*Ec*TRX), as we determined that saturation curves followed hyperbolic kinetics, with K_m values of 3.6 μM (inset

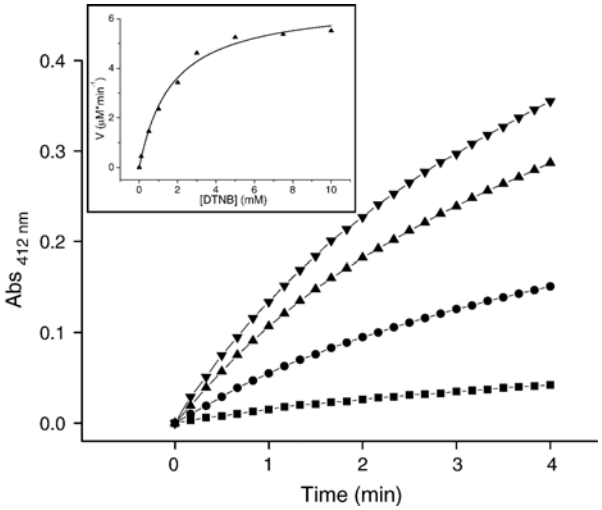

Fig. 5. DTNB reductase activity of *Eh*TRXR. The reactions were performed in buffer (100 mM phosphate, pH 7.0, 2 mM EDTA), 200 μM NADPH, 5 mM DTNB, and different concentrations of *Eh*TRXR: (■) 0.13 μM; (●) 0.33 μM; (▲) 0.53 μM; (▼) 0.66 μM. Inset: saturation curve for DTNB utilizing 0.53 μM *Eh*TRXR.

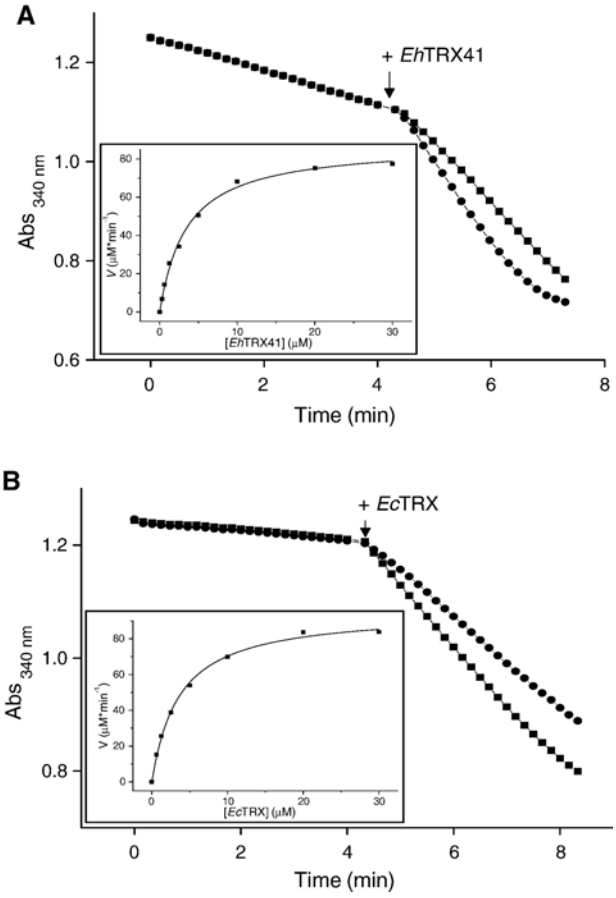

Fig. 7. Insulin reduction by TRX enzymatically reduced by NADPH and *Eh*TRXR. (A) Assay using *Eh*TRX41. The reactions were performed in buffer (100 mM phosphate, pH 7.0, 2 mM EDTA), 200 μM NADPH, 1 μM *Eh*TRXR, 130 μM insulin, and different concentrations of *Eh*TRX41: (■) 5 μM; (●) 10 μM. Inset: saturation curve for *Eh*TRX41. (B) Assay using *Ec*TRX. The reactions were performed in buffer (100 mM phosphate, pH 7.0, 2 mM EDTA), 200 μM NADPH, 1 μM *Eh*TRXR, 130 μM insulin and different concentrations of *Ec*TRX: (■) 5 μM; (●) 10 μM. Inset: saturation curve for *Ec*TRX.

Fig. 7A) and 4.6 μM (inset Fig. 7B) for *Eh*TRX41 and *Ec*TRX, respectively. A V_{max} value about 1.2 U mg^{-1} was calculated for assays performed with both of the TRXs analyzed.

The occurrence of a redox pair, TRXR/TRX, in *E. histolytica* made it relevant to investigate if it could be functional for hydroperoxide detoxification coupled with *Eh*p29, as previously proposed for the involvement of other redox proteins identified in the parasite [3]. Fig. 8 illustrates the reconstitution in vitro of such a detoxifying system, utilizing the recombinant protein components and after oxidation of NADPH by the change in absorbance at 340 nm. The addition of *t*-BOOH to a mix containing NADPH, *Eh*TRXR, and *Eh*p29 did not modify the rate of NADPH oxidation that under these conditions is due to the oxidase activity of the reductase (Fig. 8A). After the further addition to the mix of TRX (either *Ec*TRX or *Eh*TRX41) the rate of NADPH oxidation increased significantly (Figs. 8B–8D), indicating that only the entire system was able to reduce *t*-BOOH from NADPH, thus being functional for detoxification.

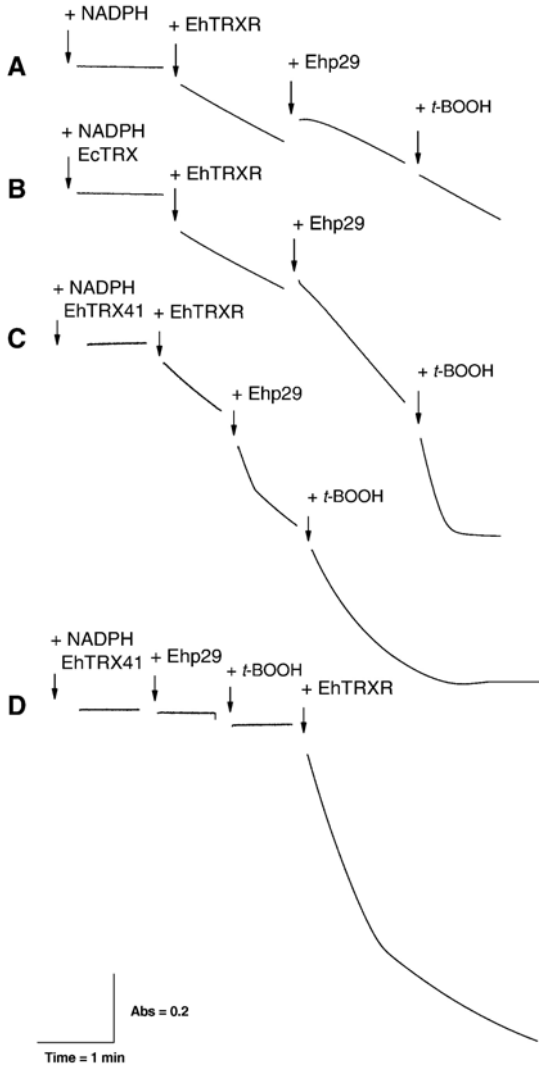

Fig. 8. Hydroperoxide detoxification activity of the oxidoreductase cascade (TRXR–TRX–peroxidase). The assay was performed in buffer (50 mM phosphate, pH 7.0, 2 mM EDTA), 300 μM NADPH, 100 μM *t*-BOOH, 1 μM *Eh*TRXR, 1 μM *Eh*p29, and (A) no TRX, (B) 10 μM *Ec*TRX, and (C) 10 μM *Eh*TRX41. The reactions were started by the addition of *t*-BOOH. In (D) the reaction was started with *Eh*TRXR.

The different variants analyzed in Fig. 8 illustrate that the effective reduction of peroxides was possible only in the presence of the complete set of molecular components: NADPH, *Eh*TRXR, TRX (*Eh*TRX or *Ec*TRX), *Eh*p29, and the peroxide. Fig. 8A shows that the oxidation of NADPH in the absence of TRX started after the addition of *Eh*TRXR, with the slope of the curve exhibiting no variations with the addition of *Eh*p29 and *t*-BOOH. When *Ec*TRX was used together with *Eh*TRXR and *Eh*p29, modifications in the slope of the curve were evidenced (Fig. 8B). The rate of NADPH oxidation increased by around twofold with the addition of *Eh*p29 and further about fourfold after addition of *t*-BOOH. Similar results were obtained when *Eh*TRX41 was used (Fig. 8C). In Fig. 8D, it is shown that the reaction was started with the addition of *Eh*TRXR and that NADPH cannot directly reduce *Eh*TRX41, *Eh*p29, or *t*-BOOH. Thus, the enzyme *Eh*TRXR identified in this work exhibited a marked difference with respect to *Eh*p34, a disulfide oxidoreductase previously characterized in *E. histolytica.* It has been reported that *Eh*p34 could transfer reduction equivalents directly to *Eh*p29 [18], whereas *Eh*TRXR needed the presence of TRX to catalyze such a reaction.

Discussion

The enteric unicellular parasite, *E. histolytica*, is the causative agent of amoebiasis, a disease that is surpassed only by malaria as a parasitic cause of death [13]. Normally resident of the large bowel, *E. histolytica* occasionally penetrates the intestinal mucosa and disseminates to other organs. A critical virulence factor of the microorganism is determined by its ability to cope with conditions of increasing oxygen pressures and high ROS concentrations [3,13,32]. Despite this, and with the scarcity of reports on the identification of molecular components, the understanding of redox metabolism in the parasite is far from complete. The current knowledge of such a metabolic scenario has been recently analyzed with the emergence of genomic data [3], as summarized in the introduction. Unexpectedly, a redox metabolism like the TRXR/TRX system, which is widespread in many organisms, was neither described nor suspected to occur in this human pathogen.

The genome of *E. histolytica* remains unfinished, its completion being a priority [33]. The current information available from The Wellcome Trust, Sanger Institute, Pathogen Sequencing Unit (http://www.genedb.org/) does not completely agree with previous reports depicting components of redox and oxygen detoxifying metabolic pathways in the parasite (specified above). Thus, the database reports sequences corresponding to the genes coding for rubrerythrin (131.m00144), FeSOD (384.m0041), *Eh*p29 (298.m00058), and flavoprotein A (sequences for four genes: 6.m00467, 65.m00171, 155.m00084, and 146.m00121). However, sequences for putative trypanothione reductase and *Eh*p34 are not found. Interestingly, in the current genome six sequences are putatively

assigned to proteins of the TRXR/TRX metabolism. Thus, two sequences (386.m00036, and 23.m00296) are found that apparently correspond to a duplicated gene for TRXR, whereas four sequences (41.m00230, 8.m00422, 111.m00121, and 6. m00418) matching genes of different TRXs are identified. This analysis highlights that the molecular components predicted to be involved in redox metabolism in *E. histolytica* need, at least, to be revisited.

Seeking to ascertain functionality of the data available in the genome of *E. histolytica* concerning the occurrence of the TRXR/TRX system, we performed the molecular cloning of genes coding for one *Eh*TRXR and for four *Eh*TRXs. Of the latter four, we expressed and purified recombinant *Eh*TRX41, a protein that conserves amino acid residues D58, G81, and cis P73, which are considered to contribute to the correct folding and modulation of the activity in TRXs [31]. It also contains residue D26, an amino acid highly conserved in other TRXs and reported to be critical for catalytic activity [34]. Importantly, *Eh*TRX41 exhibited biological activity, being able to reduce insulin. Further characterization included the expression of the *ehtrxr* gene. The structural properties of *Eh*TRXR indicate that the enzyme belongs to the low-molecular-weight family of TRXRs, having a redox active site containing two key cysteine residues. Results indicate that recombinant *Eh*TRXR possesses NADPH oxidase activity and that it is able to catalyze reduction of DTNB and also of TRX. The enzyme was active with at least one of the four TRXs found in *E. histolytica* (specifically *Eh*TRX41) and also with the protein from bacterial origin *Ec*TRX.

An alignment between the sequences of *Eh*TRXR and that of the previously reported NADPH-flavin oxidoreductase (*Eh*p34, Accession No. CAA56112) from *E. histolytica* highlights differences supporting the fact that they are different proteins (see supplemental data). The alignment points out a high level of identity (ca. 87%) between both polypeptide chains, with differences observed in regions supposedly noncritical for the protein function. Thus, *Eh*p34 primary structure contains the GVSACAICD region (amino acids 138 to 146 in the sequence of *Eh*TRXR, see supplemental data), determined to contain the two cysteine residues characteristic of and responsible for TRX reductase activity [29,35] (see also Fig. 1). Kinetically, a distinctive property found for *Eh*TRXR is that it is a true reductase of TRX and that it cannot transfer reducing equivalents directly to the *Eh*p29, as described for *Eh*p34 [18]. These results suggest that *Eh*p34 could have TRX reductase activity, a property that was not determined in the previous work carried out with this protein [3,4,15,18]. This, together with the fact that the sequence coding for *Eh*p34 is not found in the current status of the *E. histolytica* genome, makes further analysis of its differences from and similarities to *Eh*TRXR complex and speculative.

As described for other organisms, the pair TRXR/TRX could be involved in different physiological processes in *E. histolytica* such as regulation of DNA synthesis, transcription, cellular growth, and apoptosis [19–21]. Interestingly, we show in the present work that *Eh*TRXR and *Eh*TRX41 were also able to work as a redox system and, together with *Eh*p29, to catalyze the NADPH-dependent reduction of *t*-BOOH. This redox system could be functional in *E. histolytica* working as presented in Fig. 9. As shown, the detoxifying metabolism could utilize reducing power starting from NADPH to eliminate ROS in a mechanism involving *Eh*TRX that, after being reduced in a reaction catalyzed by *Eh*TRXR, reduces *Eh*p29, which finally splits peroxides to water and nontoxic organic compounds (Fig. 9). It is worth pointing out results showing that *Ec*TRX is an important partner for *Eh*TRXR (the enzyme exhibited kinetics for this substrate similar to those for *Eh*TRX). From these results, it is tempting to speculate that *Ec*TRX (or TRX from other organisms of the human intestinal microbial flora [36]) could be functional in the antioxidative machinery of the parasite. We support this proposal in previous works in which *E. histolytica* virulence was associated with the ability of the parasite to phagocytose enteric bacteria [37–39], *E. coli* being one of the inhabitants identified in the human intestine [36]. Additional support for this view is given by reports demonstrating that *Ec*TRX is a highly abundant and very stable protein [40,41] and that certain proteins from bacteria could be incorporated as functional into the parasite after phagocytosis [42].

The mechanism schematized in Fig. 9 is somehow similar to that reviewed when the *E. histolytica* genome was recently introduced [3]. However, in the present scheme we propose the involvement of proteins of the parasite that had been previously ignored and that we determined to be of potential relevance after the identification of their respective genes in the genome. Thus, the metabolic pathway shown in Fig. 9 could be complemented by the contribution of other components such as FeSOD, rubrerythrin, cysteine, flavoprotein A, *Eh*p34, or trypanothione reductase/trypanothione. Interestingly, in trypanosomatids trypanothione can alternatively reduce TRX [43], and a similar scenario could take place in *E. histolytica.* From available data, some of these molecules were already identified to occur in the parasite, whereas others are in need of the genome completion.

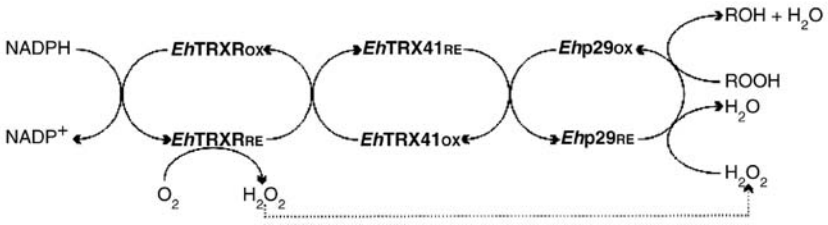

Fig. 9. Schematic description of the thioredoxin-linked hydroperoxide detoxification pathway in *E. histolytica.* ROOH, alkylhydroperoxide and H_2O_2, hydrogen peroxide.

In any case, results reported in the present work strongly suggest the occurrence of the detoxifying system proposed in Fig. 9. It would be of great value to solve definitively the complete set of reactions that are functional in *E. histolytica* to manage redox equivalents and to cope with oxidative stress, because these metabolic tools are critical for the parasite maintenance and virulence.

Acknowledgments

This work was supported by grants from ANPCyT (PICT′ 03, 1-14733; PAV′03, 137; and PICTO′03 1-13241), CONICET (PIP 6358), and UNL (CAI+D 2005). S.A.G. and A.A.I. are career investigator members from CONICET (Argentina).

Appendix A. Supplementary data

Supplementary data associated with this article can be found, in the online version, at doi:10.1016/j.freeradbiomed.2007.02.012.

References

[1] Bhattacharya, A.; Satish, S.; Bagchi, A.; Bhattacharya, S. The genome of Entamoeba histolytica. *Int. J. Parasitol.* **30:**401–410; 2000.

[2] Ondarza, R. N.; Iturbe, A.; Hurtado, G.; Tamayo, E.; Ondarza, M.; Hernandez, E. Entamoeba histolytica: a eukaryote with trypanothione metabolism instead of glutathione metabolism. *Biotechnol. Appl. Biochem.* **30**(Pt 1):47–52; 1999.

[3] Loftus, B.; Anderson, I.; Davies, R.; Alsmark, U. C.; Samuelson, J.; Amedeo, P.; Roncaglia, P.; Berriman, M.; Hirt, R. P.; Mann, B. J.; Nozaki, T.; Suh, B.; Pop, M.; Duchene, M.; Ackers, J.; Tannich, E.; Leippe, M.; Hofer, M.; Bruchhaus, I.; Willhoeft, U.; Bhattacharya, A.; Chillingworth, T.; Churcher, C.; Hance, Z.; Harris, B.; Harris, D.; Jagels, K.; Moule, S.; Mungall, K.; Ormond, D.; Squares, R.; Whitehead, S.; Quail, M. A.; Rabbinowitsch, E.; Norbertczak, H.; Price, C.; Wang, Z.; Guillen, N.; Gilchrist, C.; Stroup, S. E.; Bhattacharya, S.; Lohia, A.; Foster, P. G.; Sicheritz-Ponten, T.; Weber, C.; Singh, U.; Mukherjee, C.; El-Sayed, N. M.; Petri, W. A., Jr.; Clark, C. G.; Embley, T. M.; Barrell, B.; Fraser, C. M.; Hall, N. The genome of the protist parasite Entamoeba histolytica. *Nature* **433:**865–868; 2005.

[4] Bruchhaus, I.; Richter, S.; Tannich, E. Characterization of two E. histolytica proteins that inactivate reactive oxygen species. *Arch. Med. Res.* **28:**91–92 (Spec Issue); 1997.

[5] Choi, M. H.; Sajed, D.; Poole, L.; Hirata, K.; Herdman, S.; Torian, B. E.; Reed, S. L. An unusual surface peroxiredoxin protects invasive Entamoeba histolytica from oxidant attack. *Mol. Biochem. Parasitol.* **143:**80–89; 2005.

[6] Ariyanayagam, M. R.; Fairlamb, A. H. Entamoeba histolytica lacks trypanothione metabolism. *Mol. Biochem. Parasitol.* **103:**61–69; 1999.

[7] Fahey, R. C.; Newton, G. L.; Arrick, B.; Overdank-Bogart, T.; Aley, S. B. Entamoeba histolytica: a eukaryote without glutathione metabolism. *Science* **224:**70–72; 1984.

[8] Tamayo, E. M.; Iturbe, A.; Hernandez, E.; Hurtado, G.; de Lourdes Gutierrez, X. M.; Rosales, J. L.; Woolery, M.; Ondarza, R. N. Trypanothione reductase from the human parasite Entamoeba histolytica: a new drug target. *Biotechnol. Appl. Biochem.* **41:**105–115; 2005.

[9] Ondarza, R. N.; Hernandez, E.; Iturbe, A.; Hurtado, G.; Tamayo, E. M. Detection by HPLC of a trypanothione synthetase activity in vitro from Entamoeba histolytica. *Biotechnol. Appl. Biochem.* **30**(Pt 1):41–45; 1999.

[10] Ondarza, R. N.; Hurtado, G.; Iturbe, A.; Hernandez, E.; Tamayo, E.; Woolery, M. Identification of trypanothione from the human pathogen Entamoeba histolytica, by mass spectrometry and chemical analysis. *Biotechnol. Appl. Biochem.* **42:**175–181; 2005.

[11] Mehlotra, R. K. Parasitic protozoa: thiol-based redox metabolism. *Trends Parasitol.* **20:**58–59; 2004.

[12] Tekwani, B. L.; Mehlotra, R. K. Molecular basis of defence against oxidative stress in Entamoeba histolytica and Giardia lamblia. *Microbes Infect.* **1:**385–394; 1999.

[13] Akbar, M. A.; Chatterjee, N. S.; Sen, P.; Debnath, A.; Pal, A.; Bera, T.; Das, P. Genes induced by a high-oxygen environment in Entamoeba histolytica. *Mol. Biochem. Parasitol.* **133:**187–196; 2004.

[14] Tannich, E.; Bruchhaus, I.; Walter, R. D.; Horstmann, R. D. Pathogenic and nonpathogenic Entamoeba histolytica: identification and molecular cloning of an iron-containing superoxide dismutase. *Mol. Biochem. Parasitol.* **49:**61–71; 1991.

[15] Bruchhaus, I.; Richter, S.; Tannich, E. Removal of hydrogen peroxide by the 29 kDa protein of Entamoeba histolytica. *Biochem. J.* **326**(Pt 3):785–789; 1997.

[16] Bruchhaus, I.; Tannich, E. Analysis of the genomic sequence encoding the 29-kDa cysteine-rich protein of Entamoeba histolytica. *Trop. Med. Parasitol.* **44:**116–118; 1993.

[17] Lo, H.; Reeves, R. E. Purification and properties of NADPH:flavin oxidoreductase from Entamoeba histolytica. *Mol. Biochem. Parasitol.* **2:**23–30; 1980.

[18] Bruchhaus, I.; Richter, S.; Tannich, E. Recombinant expression and biochemical characterization of an NADPH:flavin oxidoreductase from Entamoeba histolytica. *Biochem. J.* **330**(Pt 3):1217–1221; 1998.

[19] Reckenfelderbaumer, N.; Ludemann, H.; Schmidt, H.; Steverding, D.; Krauth-Siegel, R. L. Identification and functional characterization of thioredoxin from Trypanosoma brucei brucei. *J. Biol. Chem.* **275:**7547–7552; 2000.

[20] Piattoni, C. V.; Blancato, V. S.; Miglietta, H.; Iglesias, A. A.; Guerrero, S. A. On the occurrence of thioredoxin in Trypanosoma cruzi. *Acta Trop.* **97:**151–160; 2006.

[21] Krauth-Siegel, R. L.; Bauer, H.; Schirmer, R. H. Dithiol proteins as guardians of the intracellular redox milieu in parasites: old and new drug targets in trypanosomes and malaria-causing plasmodia. *Angew. Chem. Int. Ed. Engl.* **44:**690–715; 2005.

[22] Maniatis, T. F.; Fritsch, E. F.; Sambrook, J. *Molecular Cloning: A Laboratory Manual*. Cold Spring Harbor, NY: Laboratory Press; 1982.

[23] Laemmli, U. K. Cleavage of structural proteins during the assembly of the head of bacteriophage T4. *Nature* **227:**680–685; 1970.

[24] Bradford, M. M. A rapid and sensitive method for the quantitation of microgram quantities of protein utilizing the principle of protein-dye binding. *Anal. Biochem.* **72:**248–254; 1976.

[25] Vaitukaitis, J.; Robbins, J. B.; Nieschlag, E.; Ross, G. T. A method for producing specific antisera with small doses of immunogen. *J. Clin. Endocrinol. Metab.* **33:**988–991; 1971.

[26] Holmgren, A. Thioredoxin catalyzes the reduction of insulin disulfides by dithiothreitol and dihydrolipoamide. *J. Biol. Chem.* **254:**9627–9632; 1979.

[27] Holmgren, A. Reduction of disulfides by thioredoxin: exceptional reactivity of insulin and suggested functions of thioredoxin in mechanism of hormone action. *J. Biol. Chem.* **254:**9113–9119; 1979.

[28] Bruchhaus, I.; Brattig, N. W.; Tannich, E. Recombinant expression, purification and biochemical characterization of a superoxide dismutase from Entamoeba histolytica. *Arch. Med. Res.* **23:**27–29; 1992.

[29] Coombs, G. H.; Westrop, G. D.; Suchan, P.; Puzova, G.; Hirt, R. P.; Embley, T. M.; Mottram, J. C.; Muller, S. The amitochondriate eukaryote Trichomonas vaginalis contains a divergent thioredoxin-linked peroxiredoxin antioxidant system. *J. Biol. Chem.* **279:**5249–5256; 2004.

[30] Williams, C. H.; Arscott, L. D.; Muller, S.; Lennon, B. W.; Ludwig, M. L.; Wang, P. F.; Veine, D. M.; Becker, K.; Schirmer, R. H. Thioredoxin reductase: two modes of catalysis have evolved. *Eur. J. Biochem.* **267:**6110–6117; 2000.

[31] Holmgren, A.; Soderberg, B. O.; Eklund, H.; Branden, C. I. Three-dimensional structure of Escherichia coli thioredoxin-S2 to 2.8 A resolution. *Proc. Natl. Acad. Sci. USA* **72:**2305–2309; 1975.

[32] MacFarlane, R. C.; Singh, U. Identification of differentially expressed genes in virulent and nonvirulent Entamoeba species: potential implications for amebic pathogenesis. *Infect. Immun.* **74:**340–351; 2006.

[33] Loftus, B. J.; Hall, N. Entamoeba: still more to be learned from the genome. *Trends Parasitol.* **21:**453; 2005.

[34] Dyson, H. J.; Tennant, L. L.; Holmgren, A. Proton-transfer effects in the active-site region of Escherichia coli thioredoxin using two-dimensional ^{1}H NMR. *Biochemistry* **30:**4262–4268; 1991.

[35] Hirt, R. P.; Muller, S.; Embley, T. M.; Coombs, G. H. The diversity and evolution of thioredoxin reductase: new perspectives. *Trends Parasitol.* **18:**302–308; 2002.

[36] Eckburg, P. B.; Bik, E. M.; Bernstein, C. N.; Purdom, E.; Dethlefsen, L.; Sargent, M.; Gill, S. R.; Nelson, K. E.; Relman, D. A. Diversity of the human intestinal microbial flora. *Science* **308:**1635–1638; 2005.

[37] Orozco, E.; Guarneros, G.; Martinez-Palomo, A.; Sanchez, T. Entamoeba histolytica: phagocytosis as a virulence factor. *J. Exp. Med.* **158:** 1511–1521; 1983.

[38] Rosenbaum, R. M.; Wittner, M. Ultrastructure of bacterized and axenic trophozoites of Entamoeba histolytica with particular reference to helical bodies. *J. Cell Biol.* **45:**367–382; 1970.

[39] Wittner, M.; Rosenbaum, R. M. Role of bacteria in modifying virulence of Entamoeba histolytica: studies of amebae from axenic cultures. *Am. J. Trop. Med. Hyg.* **19:**755–761; 1970.

[40] Holmgren, A.; Ohlsson, I.; Grankvist, M. L. Thiroedoxin from Escherichia coli: radioimmunological and enzymatic determinations in wild type cells and mutants defective in phage T7 DNA replication. *J. Biol. Chem.* **253:** 430–436; 1978.

[41] Gleason, F. K. Mutation of conserved residues in Escherichia coli thioredoxin: effects on stability and function. *Protein Sci.* **1:**609–616; 1992.

[42] Bracha, R.; Mirelman, D. Virulence of Entamoeba histolytica trophozoites: effects of bacteria, microaerobic conditions, and metronidazole. *J. Exp. Med.* **160:**353–368; 1984.

[43] Schmidt, H.; Krauth-Siegel, R. L. Functional and physicochemical characterization of the thioredoxin system in Trypanosoma brucei. *J. Biol. Chem.* **278:**46329–46336; 2003.